Electronic supplementary information

Improvement of *n*-butanol Guerbet condensation: a reaction integration of *n*-butanol Guerbet condensation and 1,1-dibutoxybutane hydrolysis

Xiaoxu Han[1], Shuaiqi Li[1], Hualiang An[1*], Xinqiang Zhao[1*], Yanji Wang[1]

[1] Hebei Provincial Key Laboratory of Green Chemical Technology and Efficient Energy Saving, National Local Joint Laboratory of Energy-Saving Process Integration and Resource Utilization in Chemical Industry, School of Chemical Engineering and Technology, Hebei University of Technology, Tianjin 300130, China

* Corresponding author: Dr Hualiang An: anhl@hebut.edu.cn; Prof Xinqiang Zhao: zhaoxq@hebut.edu.cn

1. Catalyst preparation

Ni-Co/HAP (Ni=12.0 wt% and Co=2.4 wt%) catalyst was prepared by the stepwise impregnation method. A nickel nitrate aqueous solution was prepared by dissolving 2.98 g $Ni(NO_3)_2 \cdot 6H_2O$ (99.9%, Alfa Company) in 100 mL deionized water. A cobalt nitrate aqueous solution was prepared by dissolving 0.5 g $Co(NO_3)_2 \cdot 6H_2O$ (99.9%, Alfa Company) in 100 mL deionized water. 5 g HAP (Acros Company, USA) was dispersed in the nickel nitrate aqueous solution and mixed thoroughly. Then the mixture was transferred into a rotatory evaporator to remove water. The resulting powder was dried at 120 °C and calcined at 400 °C for 4 h in the air to obtain NiO/HAP. After that, 5 g NiO/HAP was dispersed in the cobalt nitrate aqueous solution and mixed thoroughly. The mixture was transferred into a rotatory evaporator to remove water. The resulting powder was dried at 120 °C and calcined at 400 °C for 4 h in the air. Finally, Ni-Co/HAP catalyst was obtained after reduced at 500 °C for 4 h by a gas mixture with 80% H_2 in N_2.

TiO_2 was prepared by the sol-gel method and the specific preparation method has been described in the previous paper 0. HY (Si/Al=5.2) (analytical grade, Nankai University Catalyst Factory, China) was used after calcinated at 550 °C for 3 h.

2. Catalyst characterization

The crystalline phases of the catalyst samples were confirmed by powder X-ray diffraction (XRD) analysis on a Rigaku D/MAX-2500 X-ray diffractometer with Cu-Kα radiation. The metal loadings of the catalysts were verified by ICP analysis using a PerkinElmer Optima 7300V instrument.

3. Thermodynamic analysis of *n*-butanol Guerbet condensation reaction and its reaction integration with 1,1-dibutoxybutane hydrolysis
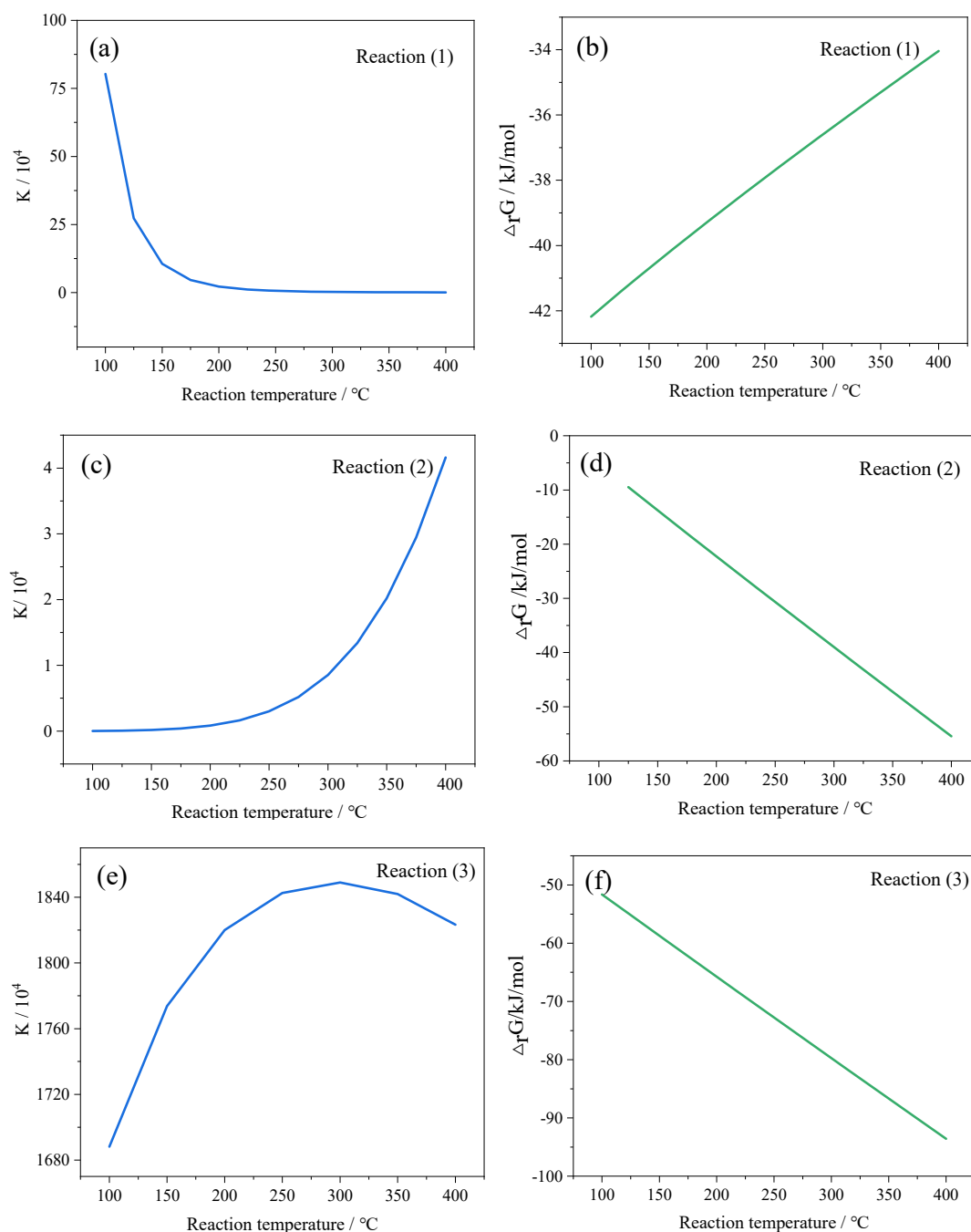
Fig. S1. *K* and $\Delta_r G$ of the different reaction at different temperatures
(a) *K* of reaction (1); (b) $\Delta_r G$ of reaction (1); (c) *K* of reaction (2); (d) $\Delta_r G$ of reaction (2); (e) *K* of reaction (3); (f) $\Delta_r G$ of reaction (3)

4. Stability of catalyst for reaction integration of *n*-butanol Guerbet condensation and 1,1-dibutoxybutane hydrolysis
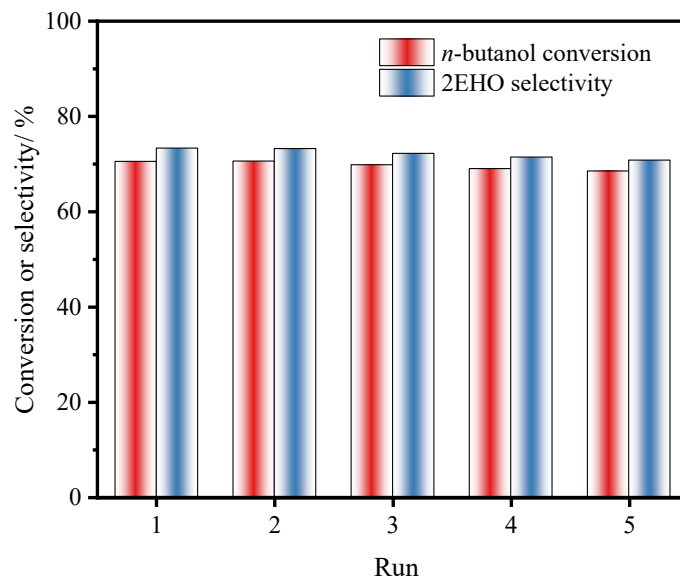
Fig. S2. Reusability of Ni-Co/HAP catalyst

Reaction conditions：Ni-Co/HAP =15wt.%, TiO_2=0.15%, n(BO): n(1,1-dibutoxybutane) =20:1, 230 ℃, 12 h.

Table S1 ICP analysis results of Ni and Co contents in Ni-Co/HAP catalyst before and after reaction

Sample	Ni content / wt.%	Co content /wt.%
Fresh	12.1	2.4
Recovered once	12.2	2.3
Recovered twice	12.2	2.1
Recovered three times	12.0	2.2
Recovered four times	12.1	2.2
Recovered five times	11.9	2.0
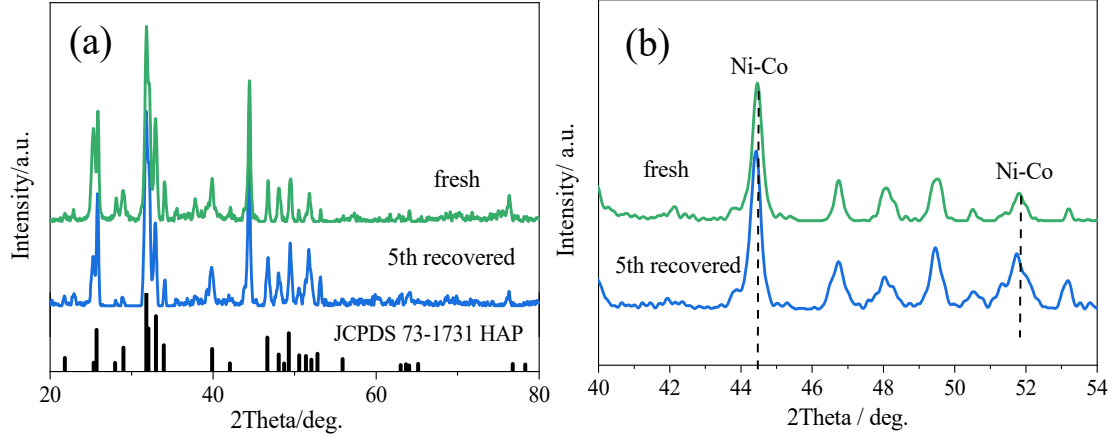
Fig. S3. XRD pattern (a) and partial enlargement (b) of fresh and recovered Ni-Co/HAP catalyst

5. Elimination of external and internal diffusion influence
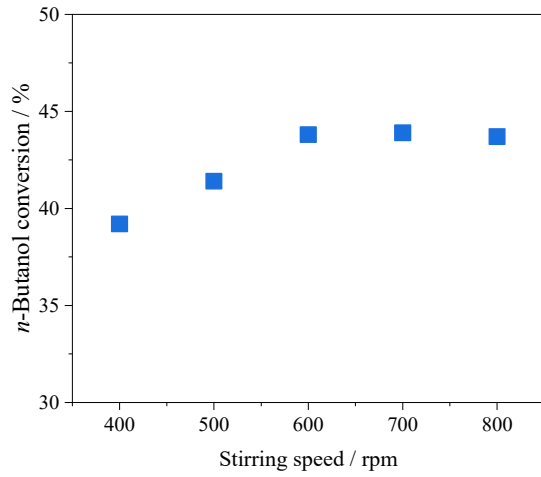
Fig. S4. Effect of stirring speed on *n*-butanol conversion
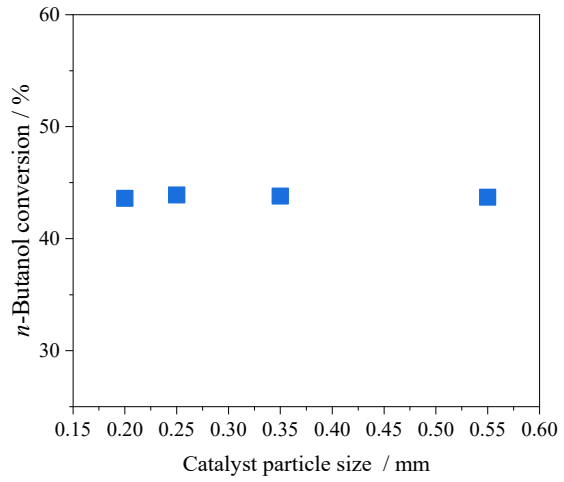
Fig. S5. Effect of particle size on *n*-butanol conversion

6. Derivation process of reaction kinetics equation

6.1 *n*-Butanol Guerbet condensation

$$r_1 = k_1 C_A^{m_1} \tag{S1}$$

$$r_1 = k_1 C_A^{m_1} \tag{S2}$$

$$r_1 = k_1 C_A^{m_1} \tag{S3}$$

The reaction rate of each component can be expressed as follows:

$$-r_A = -\frac{dC_A}{dt} = r_1 = k_1 C_A^{m_1} \tag{S4}$$

5

$$r_B = \frac{dC_B}{dt} = r_1 - r_2 = k_1 C_A^{m_1} - k_2 C_B^{m_2} \tag{S5}$$

$$r_C = \frac{dC_C}{dt} = r_2 - r_3 = k_2 C_B^{m_2} - k_3 C_C^{m_3} C_{H_2}^{m_4} \tag{S6}$$

$$r_D = \frac{dC_D}{dt} = r_3 = k_3 C_C^{m_3} C_{H_2}^{m_4} \tag{S7}$$

Where,

$$C_w = C_c + C_D \tag{S8}$$

$$C_{H_2} = C_B + C_D + 0.5C_C \tag{S9}$$

6.2 Reaction integration of *n*-butanol Guerbet condensation and 1,1-dibutoxybutane hydrolysis

$$r_1 = k_1 C_A^{m_1} \tag{S10}$$

$$r_2 = k_2 C_B^{m_2} \tag{S11}$$

$$r_3 = k_3 C_C^{m_3} C_{H_2}^{m_4} \tag{S12}$$

$$r_4 = k_4 C_E^{m_5} C_W^{m_6} \tag{S13}$$

The reaction rate of each component can be expressed as follows:

$$-r_A = -\frac{dC_A}{dt} = r_1 - r_4 = k_1 C_A^{m_1} - k_4 C_E^{m_5} C_W^{m_6} \tag{S14}$$

$$r_B = \frac{dC_B}{dt} = r_1 - r_2 + r_4 = k_1 C_A^{m_1} - k_2 C_B^{m_2} + k_4 C_E^{m_5} C_W^{m_6} \tag{S15}$$

$$r_C = \frac{dC_C}{dt} = r_2 - r_3 = k_2 C_B^{m_2} - k_3 C_C^{m_3} C_{H_2}^{m_4} \tag{S16}$$

$$r_D = \frac{dC_D}{dt} = r_3 = k_3 C_C^{m_3} C_{H_2}^{m_4} \tag{S17}$$

$$-r_E = -\frac{dC_E}{dt} = r_4 = k_4 C_E^{m_5} C_W^{m_6} \tag{S18}$$

Where,

$$C_w = C_C + C_D + C_E - C_{E0} \tag{S19}$$

$$C_{H_2} = C_B + C_D + 0.5C_C \tag{S20}$$

7. Kinetic experiments

The reaction temperature in the kinetic experiments was controlled at 210 ℃, 220 ℃ and 230 ℃. Under the conditions of a stirring speed of 600 r/min, a catalyst weight percentage of 15 wt.%, and a catalyst particle size of 0.2 to 0.15 mm, the concentration changes of each component versus reaction time at different temperatures were examined. In *n*-butanol Guerbet condensation and its reaction integration with DBB hydrolysis, the concentrations of each component versus reaction time at different temperatures are shown in Figures S6 and S7. Figure S6 shows that *n*-butanol concentration gradually decreased while the concentration of *n*-butyraldehyde and 2-ethyl-2-hexenal increased first and then slightly decreased, and the 2EHO concentration increased monotonously with the prolonging of reaction time. The concentration change trend of each component at different temperatures was basically the same.
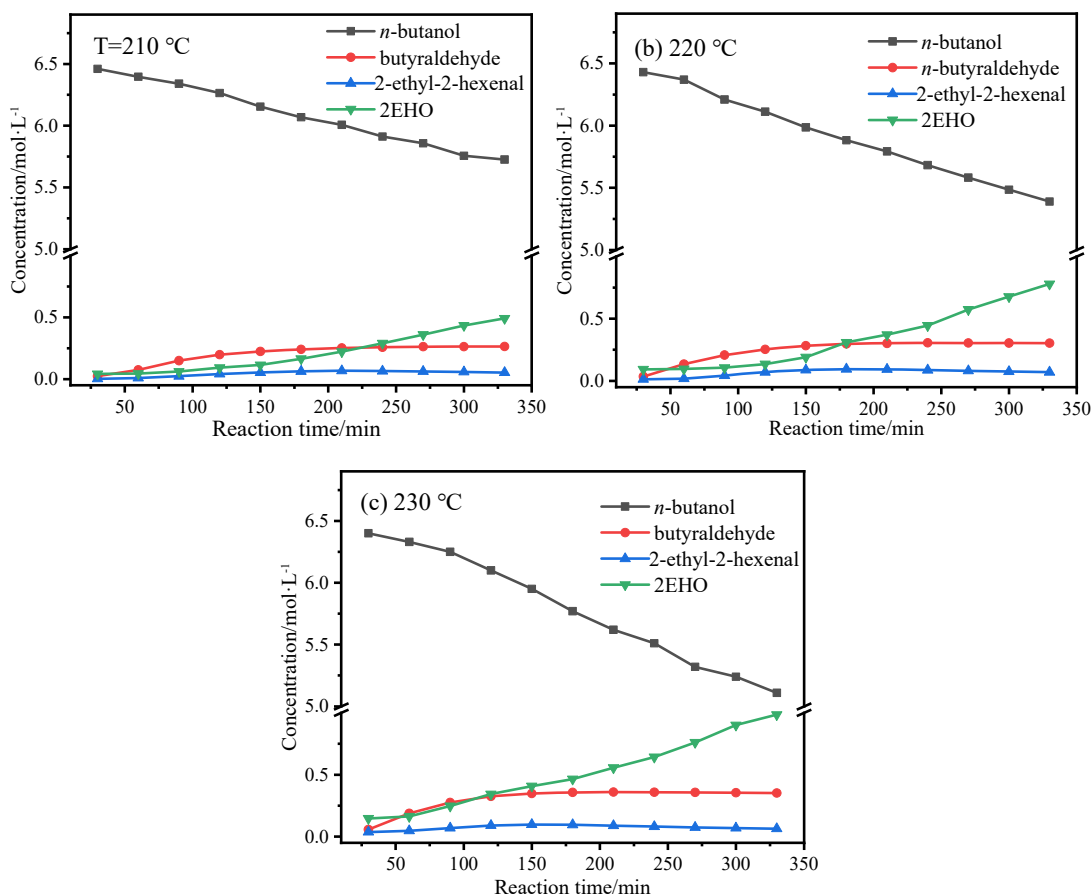
Fig. S6. Concentrations of each component in the *n*-butanol Guerbet condensation reaction at different reaction temperature versus reaction time

(a) 210 ℃；(b) 220 ℃；(c) 230 ℃

In the reaction integration of *n*-butanol Guerbet condensation and DBB hydrolysis,

the concentrations of n-butanol, *n*-butyraldehyde, 2-ethyl-2-hexenal, 2EHO and DBB changed with reaction time at different temperatures are shown in Figure S7. As can be seen, the concentration of DBB decreased monotonously until it approached to 0 at the end of the reaction. The variation trend of the concentrations of other components at different temperatures were consistent with those in the *n*-butanol Guerbet condensation.
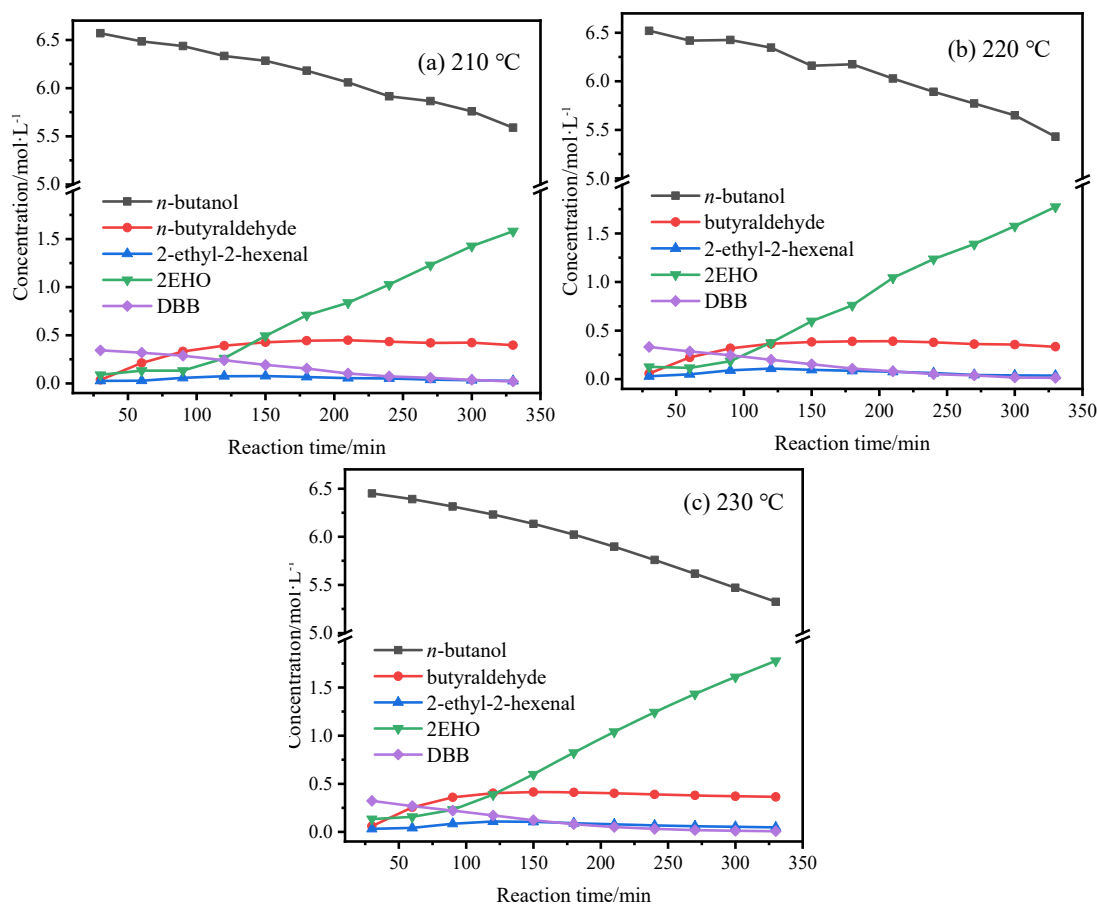
Fig. S7. Concentrations of each component in the reaction integration of *n*-butanol Guerbet condensation and DBB hydrolysis at different reaction temperature versus reaction time

(a) 210 ℃；(b) 220 ℃；(c) 230 ℃

8. Kinetic models

8.1 *n*-Butanol Guerbet condensation

The kinetic equations for *n*-butanol Guerbet condensation catalyzed by Ni-Co/HAP and TiO$_2$ are as follows.

$$-r_A = 2.38 \times 10^5 exp(\frac{-68.50 \times 10^3}{RT})C_A^{0.82}$$

$$r_B = 2.38 \times 10^5 exp(\frac{-68.50 \times 10^3}{RT})C_A^{0.82} - 2.55 \times 10^5 exp(\frac{-53.74 \times 10^3}{RT})C_B^{1.95}$$

$$r_c = 2.55 \times 10^5 exp\left(\frac{-53.74 \times 10^3}{RT}\right)C_B^{1.95} - 1.28 \times 10^4 exp(\frac{-38.24 \times 10^3}{RT})C_C^{1.12}C_{H_2}^{0.84}$$

$$r_D = 1.28 \times 10^4 exp(\frac{-38.24 \times 10^3}{RT})C_C^{1.12}C_{H_2}^{0.84}$$

8.2 Reaction integration of *n*-butanol Guerbet condensation and 1,1-dibutoxybutane hydrolysis

The kinetic equations for reaction integration of *n*-butanol Guerbet condensation and 1,1-dibutoxybutane hydrolysis catalyzed by Ni-Co/HAP and TiO$_2$ are as follows.

$$-r_A = 1.97 \times 10^4 \exp\left(\frac{-57.94}{RT}\right)C_A^{1.01} - 7.10 \times 10^3 exp(\frac{-39.67}{RT})C_E^{1.17}C_w^{0.83}$$

$$r_B = 1.97 \times 10^4 \exp\left(\frac{-57.94}{RT}\right)C_A^{1.01} - 7.20 \times 10^4 \exp\left(\frac{-47.63}{RT}\right)C_B^{1.98}$$

$$+7.10 \times 10^3 exp(\frac{-39.67}{RT})C_E^{1.17}C_w^{0.83}$$

$$r_C = 7.20 \times 10^4 exp(\frac{-47.63}{RT})C_B^{1.98} - 1.49 \times 10^4 exp(\frac{-38.37}{RT})C_C^{1.02}C_{H_2}^{0.93}$$

$$r_D = 1.49 \times 10^4 exp(\frac{-38.37}{RT})C_C^{1.02}C_{H_2}^{0.93}$$

$$-r_E = -7.10 \times 10^3 exp(\frac{-39.67}{RT})C_E^{1.17}C_w^{0.83}$$

9. Test of kinetic models

9.1 *n*-butanol Guerbet condensation

T=210 °C
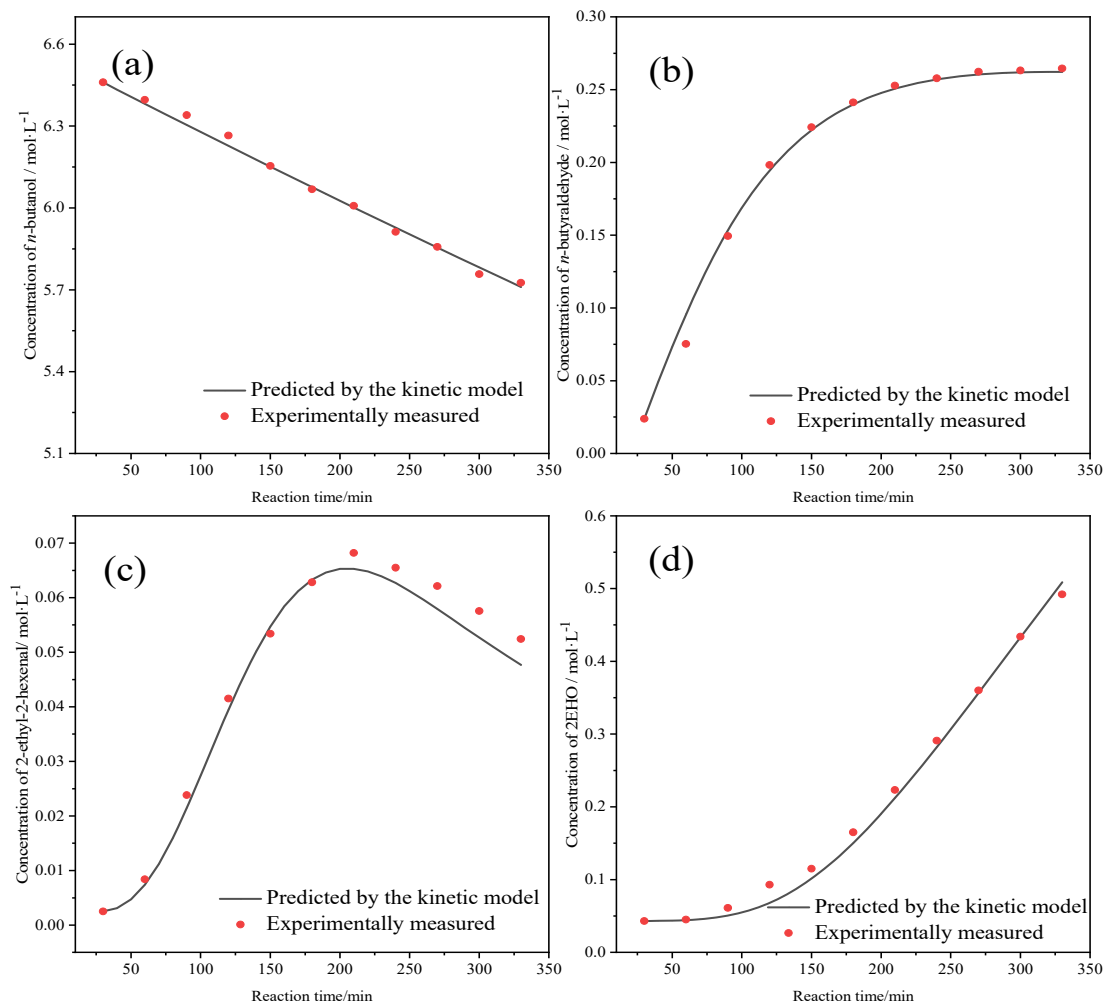
Fig. S8. Comparison of experimentally measured concentrations with those predicted by kinetic models at 210 °C
(a) Concentration of *n*-butanol; (b) concentration of *n*-butyraldehyde; (c) concentration of 2-ethyl-2-hexenal; (d) concentration of 2EHO

T=220 °C
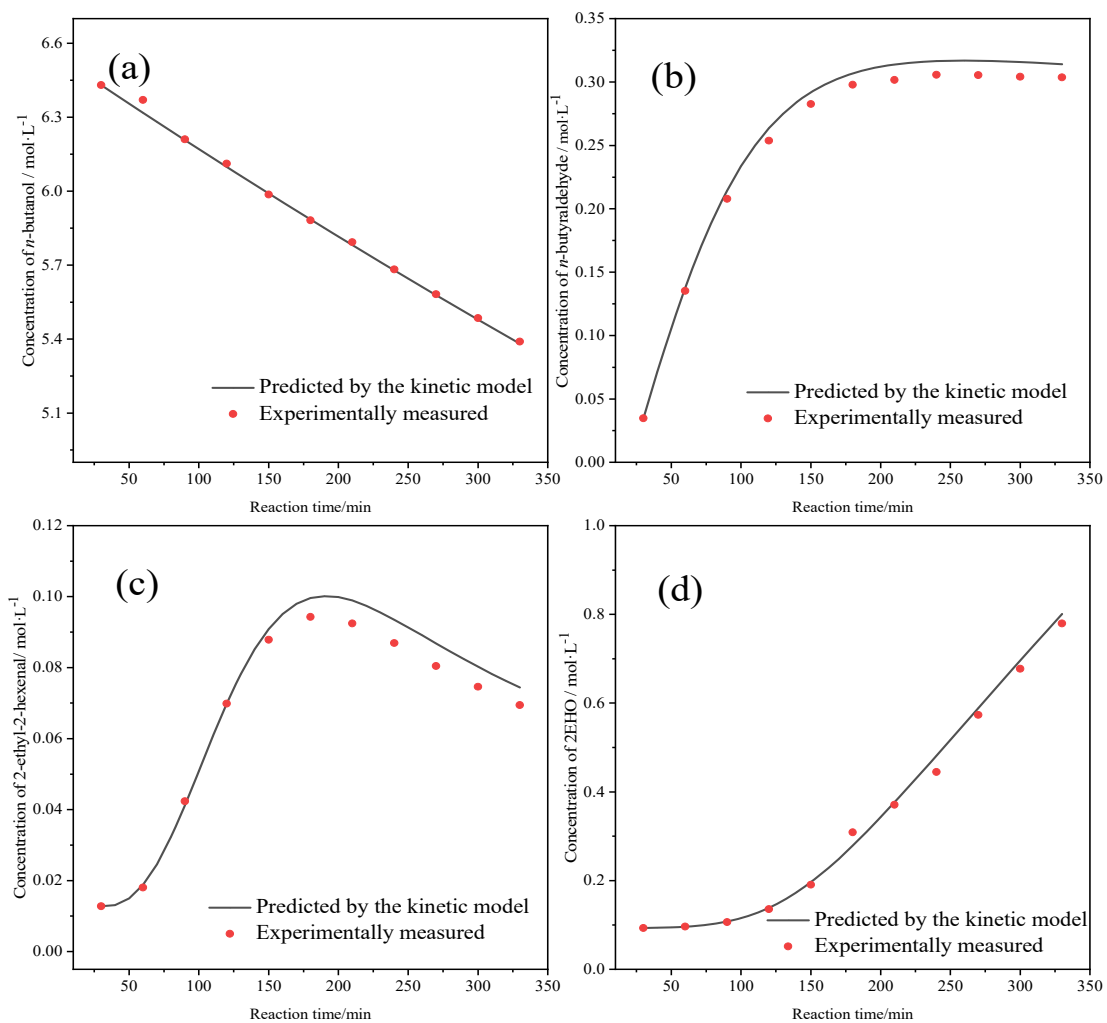
Fig. S9. Comparison of experimentally measured concentrations with those predicted by kinetic models at 220 °C
(a) Concentration of *n*-butanol; (b) concentration of *n*-butyraldehyde; (c) concentration of 2-ethyl-2-hexenal; (d) concentration of 2EHO

T=230 ℃
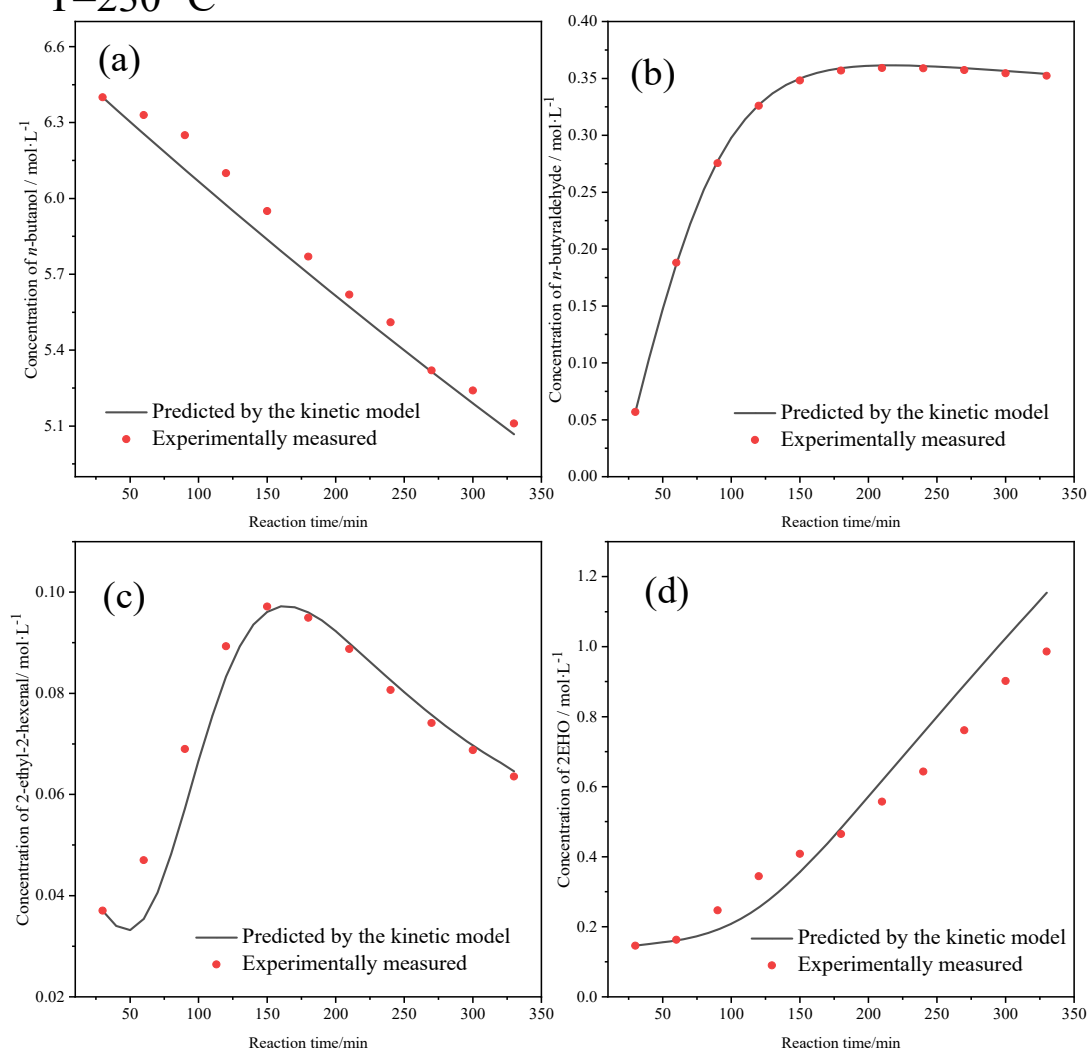
Fig. S10. Comparison of experimentally measured concentrations with those predicted by kinetic models at 230 ℃
(a) Concentration of *n*-butanol; (b) concentration of *n*-butyraldehyde; (c) concentration of 2-ethyl-2-hexenal; (d) concentration of 2EHO

Table S2 Model Statistics

Model	Reaction temperature /°C	Experiment No.	Free variation No.	Regression square sum	Residual squares sum	Correlation index	F
I	210	11		0.6181	0.0042	0.9977	
	220	11	3	1.2107	0.0032	0.9991	5671.1
	230	11		2.0021	0.0684	0.9957	
II	210	11		0.0633	0.0005	0.9976	
	220	11	3	0.0870	0.0009	0.9999	50763.1
	230	11		0.0960	0.0003	0.9999	
III	210	11		0.0052	0.0001	0.9962	
	220	11	3	0.0100	0.0002	0.9981	1199.4
	230	11		0.0046	0.0003	0.9720	
IV	210	11		0.2819	0.0016	0.9986	
	220	11	3	0.6604	0.0033	0.9985	3999.0
	230	11		1.3382	0.0898	0.9924	

I: Rate equation (r_A); II: Rate equation (r_B); III: Rate equation (r_C); IV: Rate equation (r_D).

9.2 Reaction integration of *n*-butanol Guerbet condensation and 1,1-dibutoxybutane hydrolysis

T= 210 ℃
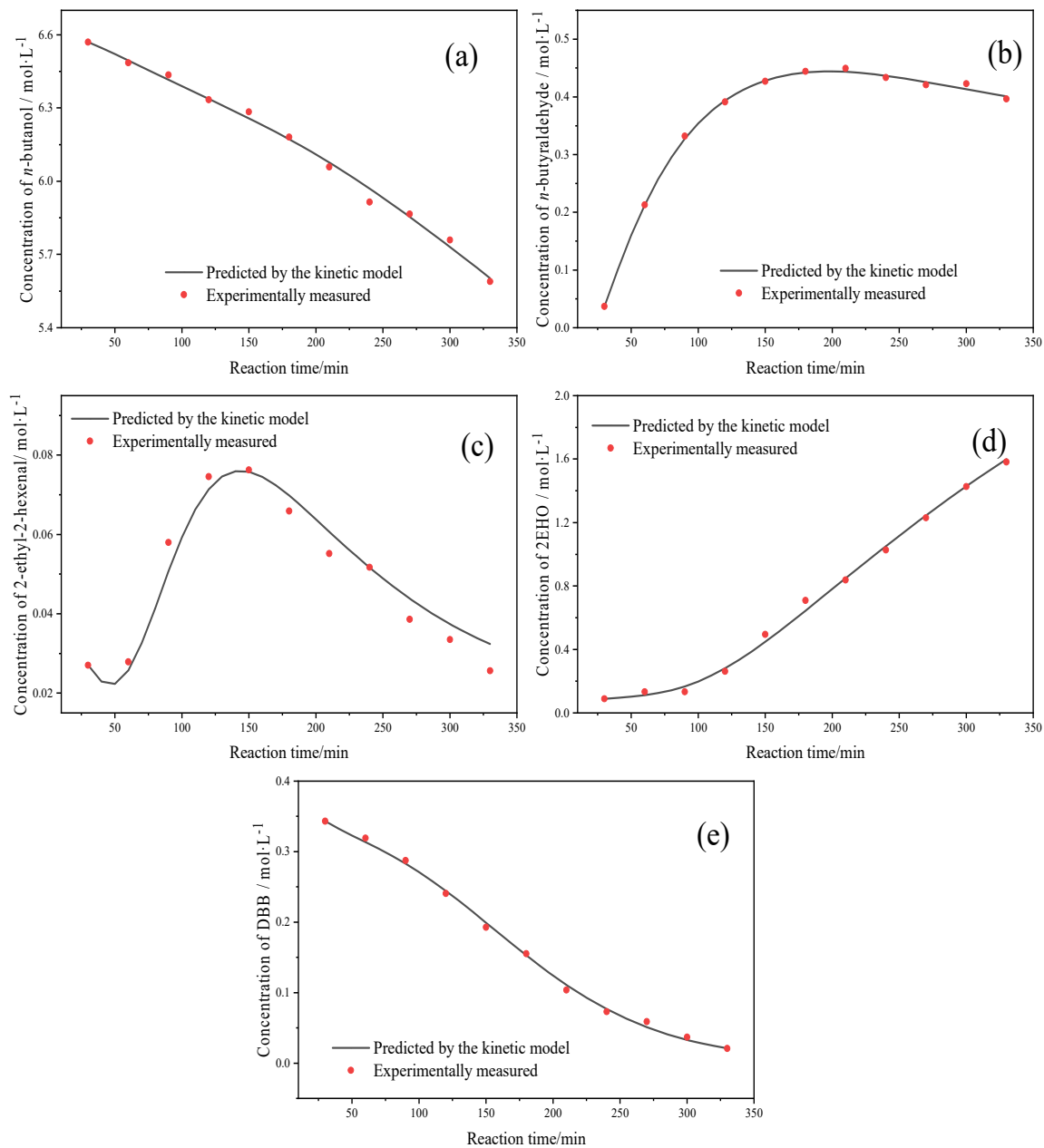
Fig. S11. Comparison of experimentally measured concentrations with those predicted by kinetic models at 210 ℃

(a) Concentration of *n*-butanol; (b) concentration of *n*-butyraldehyde; (c) concentration of 2-ethyl-2-hexenal; (d) concentration of 2EHO; (e) concentration of DBB

T= 220 °C
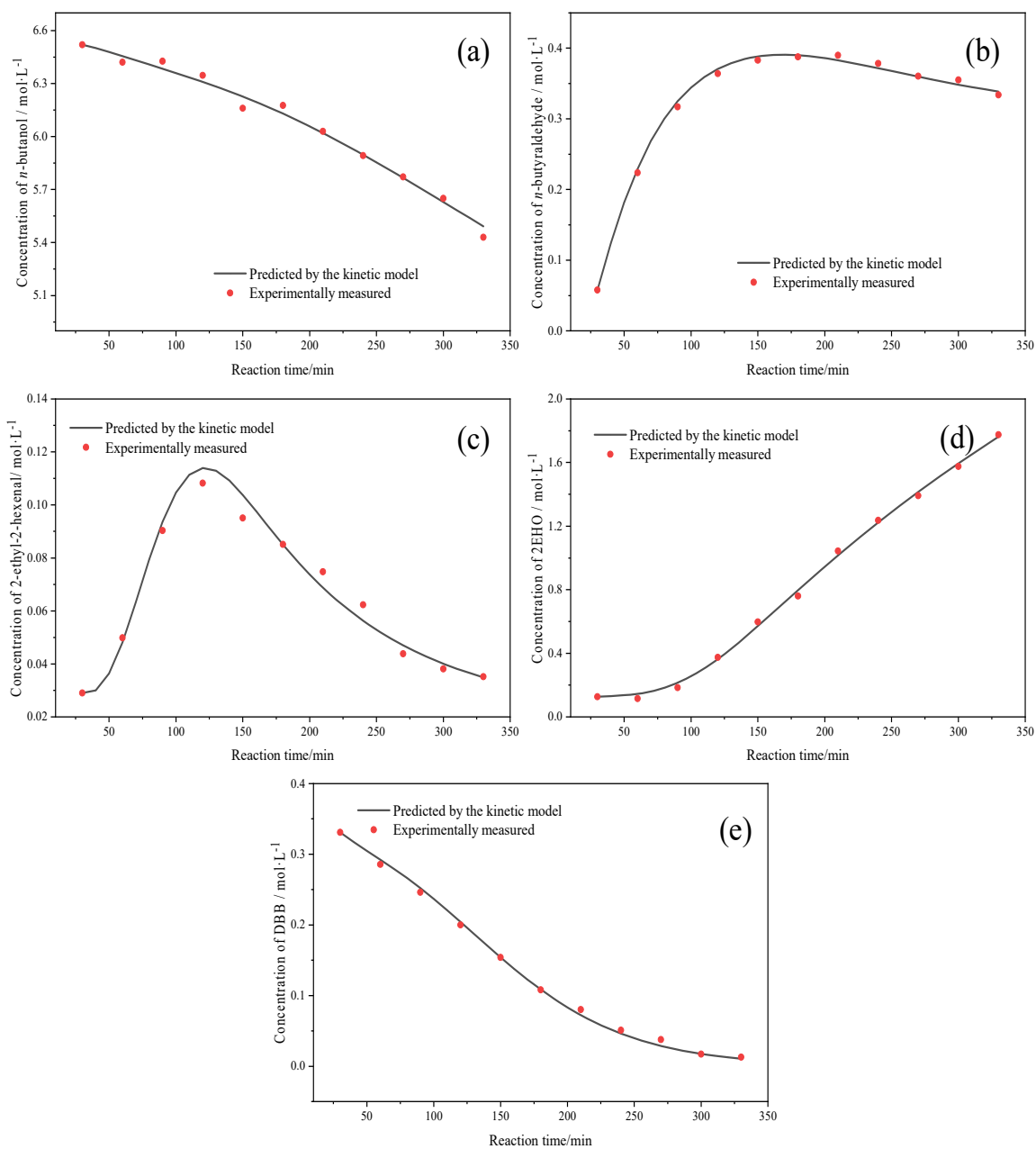
Fig. S12. Comparison of experimentally measured concentrations with those predicted by kinetic models at 220 °C
(a) Concentration of *n*-butanol; (b) concentration of *n*-butyraldehyde; (c) concentration of 2-ethyl-2-hexenal; (d) concentration of 2EHO; (e) concentration of DBB

T= 230 °C
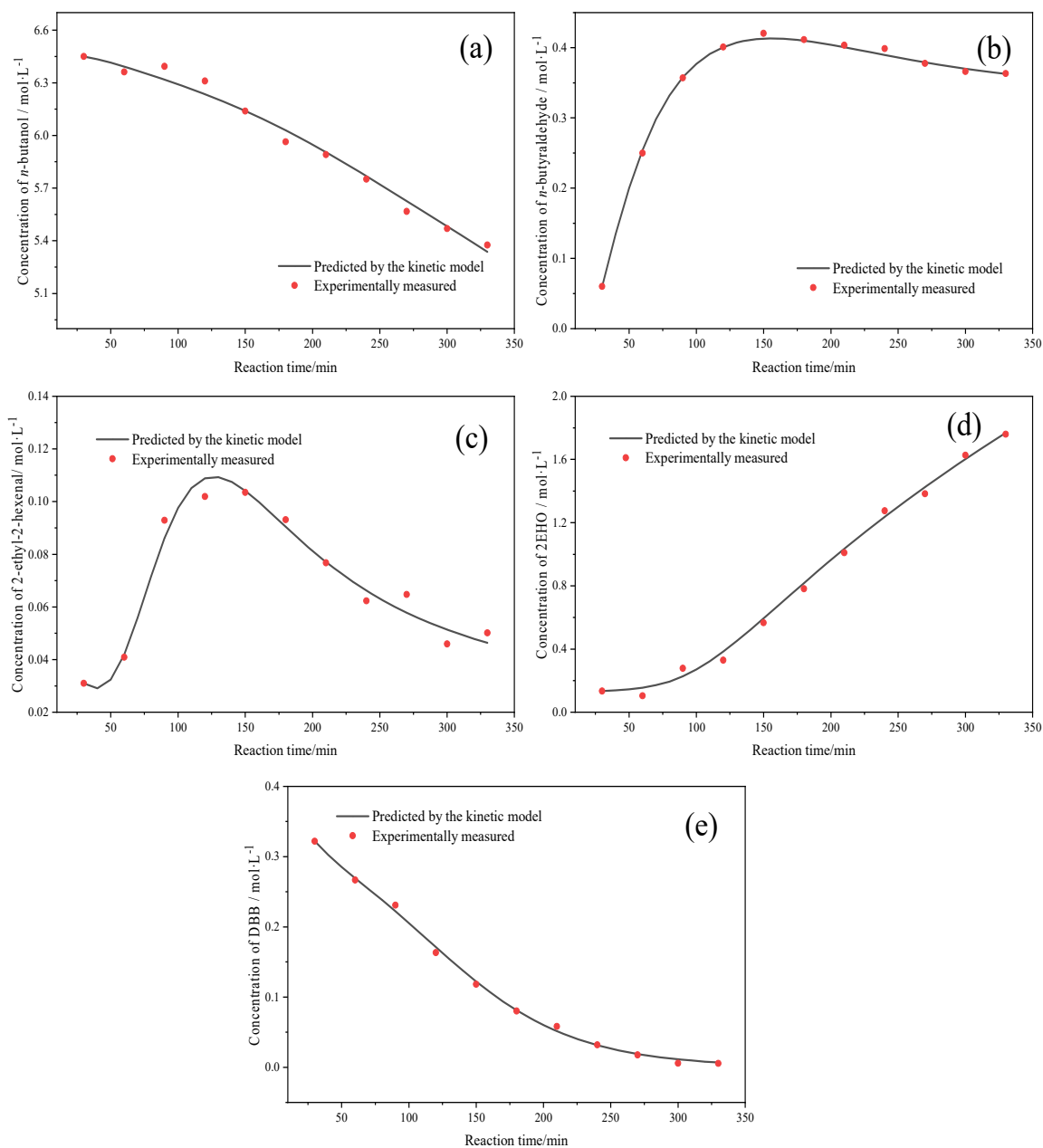
Fig. S13 Comparison of experimentally measured concentrations with those predicted by kinetic models at 230 °C
(a) Concentration of *n*-butanol; (b) concentration of *n*-butyraldehyde; (c) concentration of 2-ethyl-2-hexenal; (d) concentration of 2EHO; (e) concentration of DBB

Table S3 Model Statistics

Model	Reaction temperature /°C	Experiment No.	Free variation No.	Regression square sum	Residual squares sum	Correlation index	F
I	210	11		1.0114	0.0058	0.9972	3242.64
	220	11	3	1.1894	0.0152	0.9942	
	230	11		1.4338	0.0222	0.9930	
II	210	11		0.1614	0.0002	0.9993	
	220	11	3	0.0983	0.0003	0.9984	17149.48
	230	11		0.1086	0.0002	0.9993	
III	210	11		0.0033	0.0002	0.9741	
	220	11	3	0.0086	0.0002	0.9899	955.78
	230	11		0.0068	0.0002	0.9845	
IV	210	11		3.0223	0.0096	0.9985	
	220	11	3	3.6098	0.0059	0.9992	11902.91
	230	11		3.5902	0.0151	0.9982	
V	210	11		0.1371	0.0003	0.9991	
	220	11	3	0.1350	0.0003	0.9995	15660.44
	230	11		0.1250	0.0002	0.9991	

I: Rate equation (r_A); II: Rate equation (r_B); III: Rate equation (r_C); IV: Rate equation (r_D); V: Rate equation (r_E).

References

[S1] S. Li, X. Zhu, H. An, X. Zhao, Y. Wang, Ethanol Guerbet condensation to *n*-butanol or C4-C8 alcohols over Ni/TiO$_2$ catalyst[J]. ChemistrySelect. 5 (2020) 8669-8673. https://doi.org/10.1002/slct.202001063.